JOURNAL OF MATERIALS SCIENCE 31 (1996) 1693–1702

Magnetic domain refinement of silicon–steel laminations by laser scribing

S. PATRI, R. GURUSAMY, P. A. MOLIAN, M. GOVINDARAJU*
*Mechanical Engineering Department, and * Ames Laboratory, Iowa State University, Ames, IA 50011, USA*

Laser scribing of 3% silicon steel laminations was carried out using three different lasers: a KrF excimer laser, a pulsed Nd:YAG laser and a continuous wave CO_2 laser. The processing parameters included the energy fluence at the surface of the workpiece, pulse repetition rate and pulse separation distance (for the pulsed lasers), scan separation distance and scan direction. The samples were tested for hysteresis loss, permeability, coercivity, remanence and saturation induction before and after laser treatment. An overall improvement in the core loss was observed in the laser-scribed samples. The best improvement in core loss was obtained in excimer laser scribing on the rolling direction and CO_2 laser scribing in the transverse direction. Three mechanisms were proposed to explain the improvement in energy efficiency characteristics of the silicon–steel samples: magnetic domain refinement, stress relaxation and inhibition of domain-wall movement. Domain refinement, namely the formation of subdomains, results from the shocks induced by the beam. Laser scribing also relieves the stresses that are induced in the material during manufacture. The scribe lines increase the surface resistivity of the material, resulting in reduced eddy current loss. Tensile stresses are created between the laser scribe lines that elongate the domains and serve to refine the domain-wall spacing thus inhibiting the wall movement and reducing core losses.

1. Introduction

Soft ferromagnetic materials find numerous applications as a result of their ability to enhance the magnetic flux produced by an electrical current. The applications include electrical power generation and transmission equipment (transformer cores, motor armatures, etc.), electromagnets, receivers of radio and microwave signals, inductors and relays. The market for soft magnetic materials is currently $3.5 billion per year out of a total magnetic materials market of $8 billion per year. Within the soft magnetic materials market, silicon–iron comprises 85% of the total, soft ferrites comprise 10%, and the remaining 5% is shared between the nickel–iron alloys (permalloys) and a new group of materials known as amorphous alloys [1, 2]. Transformer cores are generally manufactured from laminated sheets of metal to prevent losses due to eddy current circulation to the core. The efficiency of the core material depends on core geometry, core material, surface insulation and mechanical stresses in the core.

Core loss is a measure of the resistance to the transference of magnetic flux through the core. There are three different forms of core losses: the d.c. hysteresis loss P_H, which is determined from the d.c. magnetization curve and is primarily a function of microstructure; the classical eddy current loss, P_c, which is calculated on a continuum basis, and depends on the permeability and conductivity of material; and the anomalous loss, P_A, governed by the magnetic domain-wall dynamics, which is principally dependent on the rate of change of magnetic induction [3, 4].

The total core loss can therefore be expressed as $P_{total} = P_H + P_c + P_A$. The relative contributions of these losses is, of course, dependent on a variety of conditions but, in general, $P_H > P_A > P_c$ which implies that the microstructural effects and the field excitation effects dominate over the chemical composition effects. The hysteresis loss is controlled through manipulation of microstructure and relief of internal stresses through heat treatment such as furnace or laser annealing while the anomalous loss can be minimized by controlling the magnetic field excitation wave form.

The factors that affect the core loss to an appreciable extent are [5]: orientation and size of grains; the presence of inclusions and purity of the material; internal strains; thickness of the laminations; silicon content (if the material is silicon–steel); degree of refinement of the magnetic domains; surface tension on the laminate. Of these factors, those which can be modified after manufacture of the material are the degree of refinement of the magnetic domains, and internal strains. The magnetic domains can be refined by heat-treatment methods such as conventional furnace annealing, or by laser irradiation. The objective of

0022–2461 © *1996 Chapman & Hall*

the present study was to evaluate the effect of laser scribing on the magnetic domain refinement of silicon–steel laminations.

Lasers have been used extensively for materials processing applications since their invention in 1960. Some of their applications include cutting, welding and drilling of metals; cutting of plastics, composites, paper, cloth; surface hardening of gear teeth and cutting tools, etc. A relatively new application of lasers is scribing of materials, where only the surface properties are to be modified. Laser scribing refers to removal of a thin layer of material from the surface. Scribing is used to generate grooves on the surface of the workpiece. Scribing requires tight beam focusing at the work surface and precise control of pulse power and shape. The key to improving scribing efficiency and quality is not the level of absolute power a laser produces, but the spatial and temporal profile of the laser beam at the work surface. The material used for the cores of transformers in electrical transmission equipment is in the form of thin ribbons, which is stacked in the form of laminations. These ribbons are typically about 0.05–1 mm thick, and 3–8 mm wide. As such, these materials are excellent candidates for laser scribing because the magnetic properties of these materials depend on the domain structure at the surface.

Prior to describing the desirable properties of a core material, it is useful to provide a brief nomenclature of the magnetic properties of ferromagnets. The macroscopic magnetic properties are best represented by a plot of magnetic induction, B, versus field strength, H, known as a hysteresis loop. A typical B–H hysteresis loop is shown in Fig. 1 from which five useful magnetic properties, listed below, can be obtained.

1. Permeability, μ, given by the ratio B/H, is probably the most important single property in engineering applications, because high μ is required to obtain high B for a given H, to permit retention of magnetization, and to act as a source of field to produce torque in electric motors [6]. For ferromagnetic materials, μ is not constant and varies along the B–H curve. The maximum differential permeability, μ_{max}, measured at the coercive point $H = H_c$, $B = 0$, will be used in this study as an indicator of permeability.

2. Power loss or hysteresis loss, W_c, is the area enclosed by the loop and represents the energy expended during one cycle. For a.c. applications, W_c should be as low as possible.

3. Coercivity, H_c, is one-half of the width of the loop across the H-axis and is the magnetic field needed to reduce the magnetization to zero.

4. Remanence, B_r, is the remaining magnetic induction when the field is reduced to zero after the material is magnetized. It is measured as the height of the curve along the B-axis when $H = 0$.

5. Saturation magnetic induction, B_s, is the upper limit to the magnetic induction that can be achieved when H is increased.

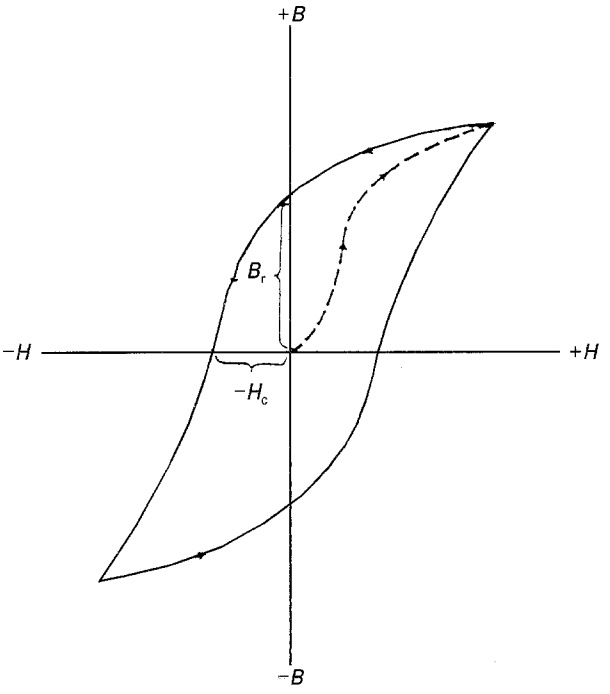

Figure 1 A typical B–H loop of magnetic material.

2. Materials and methods

2.1. Silicon–steel

Silicon–steels, as mentioned before, form the single largest segment of the soft magnetic materials market. They are currently manufactured in two varieties: non-oriented and grain-oriented. The non-oriented grades are typically produced in strips up to 1300 mm wide and between 0.35 m and 0.8 mm thick [7]. The steel is cold-rolled in several passes. Intermediate annealing is also performed to produce a large grain structure which gives a high permeability and low hysteresis loss. However, care must be taken not to exceed a grain size of about 1 mm diameter, because beyond this size, anomalous eddy current loss predominates and the total core loss increases. Thus the cold-rolling process in combination with the intermediate annealing controls the final losses and permeability, while the earlier hot-rolling process produces the required random grain orientation. The strips are usually coated with an organic or inorganic coating that provides interlaminar insulation during use. The silicon content of these steels normally ranges from 0%–3%.

Grain-oriented steels are produced in widths up to 1.27 m and between 0.23 and 0.35 mm thick. The hot-rolled strip is annealed to remove surface oxides and is cold-rolled to about 0.6 mm thickness. This is followed by another anneal to recrystallize the cold-worked structure before cold-rolling again to the final gauge. A decarburization process to reduce the carbon content to less than 0.003% is followed by annealing at 1473 K to induce the crystallization of large grains with [0 0 1] directions, close to the rolling direction. Manganese sulphide is used as an additive to suppress the growth of grains having other orientations. Grain-oriented steels have a silicate and phosphate coating which affects the final magnetic properties of the material. They can be further subdivided into two grades, a high-permeability form with improved texture

TABLE I Magnetic properties of grain-oriented and non-oriented silicon steels

Steel type	W_c(W kg^{-1})	B_s(T)	μ_{max}	H_c(Oe)
Non-oriented	3.48	1.99	500	0.70
Grain-oriented	1.45	2.00	> 1800	0.09

TABLE II Comparison of grain-oriented and non-oriented silicon steels

Parameter	Grain-oriented	Non-oriented
Width (m)	1.27	1.3
Thickness (mm)	0.23–0.35	0.35–0.8
Silicon content (%)	2.9–3.2	0–3
Core loss at 1.5 T, 50 Hz (W kg^{-1})	0.89	1.5
Induction at 1 Oe (T)	1.62	1.1
Coating	Phosphate/silicate	Phosphate/chromate compounds

and coating, and a high-performance domain-refined grade. The silicon content of grain-oriented steels varies from 2.9%–3.2%. The higher the silicon content, the better is the performance of electrical steels, because a higher silicon content increases resistivity, anisotropy and magnetostriction. But it also decreases saturation magnetization and permeability, and makes the steel brittle.

Table I shows the magnetic properties of 3% silicon steel, both the non-oriented and the grain-oriented types. Table II shows a comparison of grain-oriented and non-oriented silicon steels [8]. In the present work, we have used non-oriented steel. Silicon–iron (3% Si) samples were received from Asea Brown Boveri Technology Corporation, Raleigh, NC. The sample dimensions were 0.3 m long by 0.03 m wide by 0.35×10^{-3} m thick. The samples were coated with a phosphate coating 10 μm thick.

2.2. Lasers

Three different lasers were used to scribe the silicon steel samples in this study; carbon dioxide, Nd:YAG and excimer, the specifications of which are shown in Tables III–V.

2.3. Laser scribing

The scribing process involved scanning the beam on the sample surface with the aid of an X–Y table. The beam was stationary and was incident normal to the sample surface. The samples were irradiated either in longitudinal (lengthwise) or transverse (widthwise) direction. The experimental variables were the pulse energy and pulse repetition rate (for excimer and Nd:YAG lasers), the velocity of the X–Y table, the distance between scribe lines and the scribe direction. The ratio of the velocity of the X–Y table to the repetition rate gives the laser pulse separation on the surface of the sample. Two scribe directions were used: as-rolled (AS) and perpendicular to the as-rolled direction (XAS). Only XAS type samples were investigated with the carbon dioxide laser.

TABLE III Excimer laser specifications

Model	Lambda Physik, Model 110 i
Pulse energy (mJ)	400 mJ maximum
Pulse rate (Hz)	1–100
Wavelength (nm)	248, UV
Pulse width (ns)	23 ± 3%
Beam size (mm)	10 × 20

TABLE IV Nd:YAG laser specifications

Model	Wec Corp, W-770-Y2
Pulse energy (J)	0.5–0.6
Pulse rate (Hz)	1, 5, 10
Wavelength (nm)	1064
Pulse width (ms)	0.3

TABLE V CO_2 laser specifications

Model	Spectra Physics, Model 820
Operating mode	Continuous wave
Power range (W)	200–2000
Wavelength (nm)	10600

2.4. Magnetic measurements

Following the laser treatment, the magnetic properties of the samples were measured using a conventional fluxmeter device, where a sinusoidally varying field $H(t) = H_0 \sin(2\pi ft)$, where t is time, f is frequency (50 Hz) and H_0 is the initial field amplitude. The laser-processed samples were characterized both in a.c. and d.c. fields. A Phillips PM-550 waveform synthesizer generated a sine wave at a fixed frequency of 50 Hz and variable amplitude under computer control. The synthesizer output, amplified in power by a Kepco 36-6M power amplifier, was fed into a solenoid to produce an alternately cycling (a.c.) magnetic field at 50 Hz along its axis. The response of the sample placed longitudinal to the axis of solenoid was picked up by a fine coil wound tightly around the sample. The signal generated in the coil was amplified and digitized using a LeCroy 9314M digitizing oscilloscope, also connected to the computer. Digitized response of the sample to the a.c. magnetic field was transferred to the computer from the oscilloscope for calculation of its magnetic parameters and for further analysis. Demagnetization errors involved with samples of small aspect ratio were avoided by using sample dimensions of 0.15 m × 0.013 m, for an aspect ratio of 12. The magnetizing solenoid, consisting of 1450 turns, was 0.23 m long and had a diameter of 0.064 m. The pick-up coil wound on a non-magnetic former closely fitting the sample consisted of 2000 turns and had a cross-section of 0.1×10^{-4} m^2.

Characterization of the silicon–steel samples under d.c. magnetic field was performed using a Magnescope,

a device developed by Ames Laboratory, US Department of Energy, Ames, IA, for measurement of magnetic properties of samples with standard dimensions. The samples were wound with a pick-up coil of fine copper wire half-way along their length. The number of turns in the pick-up coil is determined by other instrument settings. Usually, 38 turns were used. A Hall probe is positioned on the sample such that its tip lies just beside the pick-up coil. The sample is then placed inside a solenoid which is then energized by a direct current. The two ends of the pick-up coil are connected to the Magnescope. The sample is first demagnetized and then magnetized until the magnetic flux density reaches saturation. The data acquired from the pick-up coil are then transferred to the software which calculates the hysteresis loss, remanence, coercivity and permeability of the sample.

A.c. characterization was performed using a standard fluxmeter configuration consisting of fluxmeter, Gaussmeter, solenoid and oscilloscope, shown schematically in Fig. 2. The solenoid is energized using a.c. Five different magnetic induction levels were used in the characterization: 0.8, 0.9, 1.0, 1.1 and 1.4 T. The reason for this is because the XAS samples could not be magnetically saturated up to 1.4 T owing to the orientation of their magnetic domains. A lock-in amplifier was used to compare the susceptibility of the samples scribed with the laser with that of the untreated samples. The amplifier was used in conjunction with the fluxmeter configuration shown in Fig. 2. The voltage on the lock-in amplifier was taken as a measure of the susceptibility.

3. Results and discussion

Magnetic properties can be enhanced by refining the domain size as well as the domain-wall spacing. Smaller domains lend themselves much more easily to magnetization; eddy current losses are also smaller for smaller-sized domains. Magnetic properties can also be modified by controlling the pinning sites such as dislocations, grain boundaries, inclusions and precipitates, and by the applied stress. The magnetic domain theory infers that the stress field associated with the imperfections impedes the motion of the domain walls and thereby increases the coercivity and hysteresis loss but decreases permeability. By relieving this stress field, improved magnetic properties may be obtained. Stress relief is performed by a laser scribing technique in this study. The aim of this study was to reduce the core losses and increase permeability, both of which are essential for efficient conversion of electrical energy. For electromagnetic applications, the material needs to have low remanence and low coercivity to ensure that the magnetization can be easily reduced to zero, and also high permeability to enable high induction to be achieved.

3.1. Excimer laser scribing

Laser-scribing variables were the energy per pulse of the laser beam, the pulse separation distance and the distance between the scribe lines. The data on the process variables are shown in Table VI. The samples were characterized under an a.c. field before and after laser treatment.

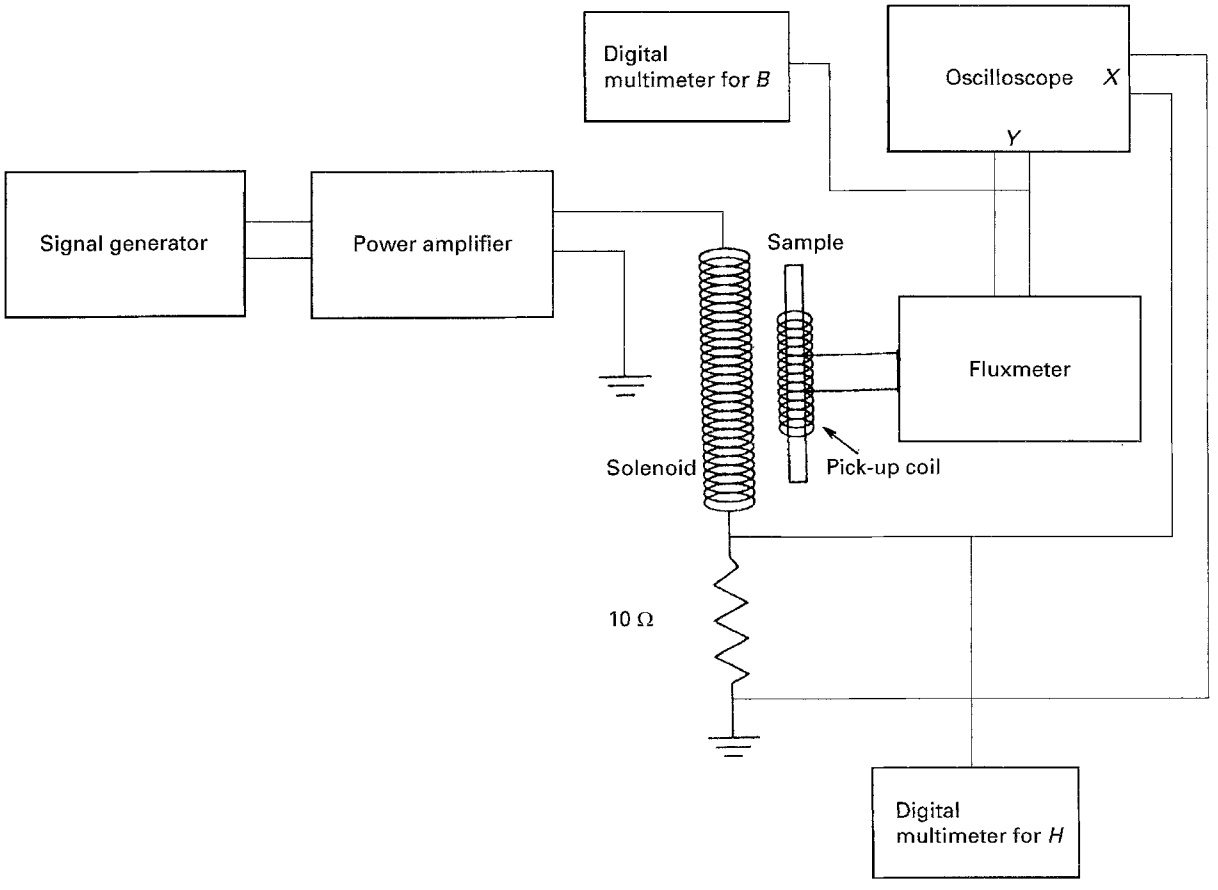

Figure 2 Schematic representation of the fluxmeter configuration.

TABLE VI Excimer laser scribing of 3% silicon–steel

Laser	KrF excimer (248 nm)
Pulse energy (mJ)	100
Pulse repetition rate (Hz)	5, 9, 10
Speed of XY table (mm s^{-1})	12,7, 41.3
Scan separation distance, (mm)	1.27–10.16
Domain orientation	AS

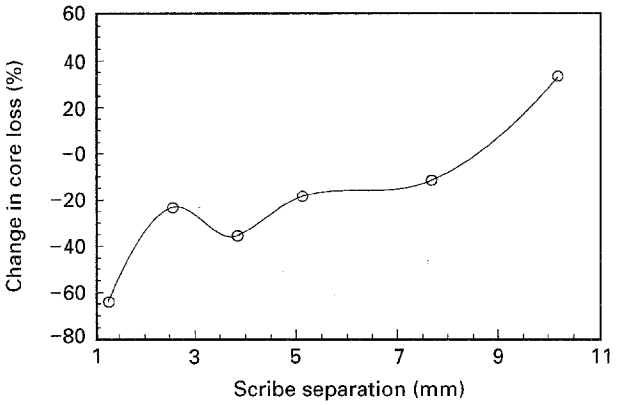

Figure 3 Per cent change in core loss of 3% silicon–steel, widthwise scribing.

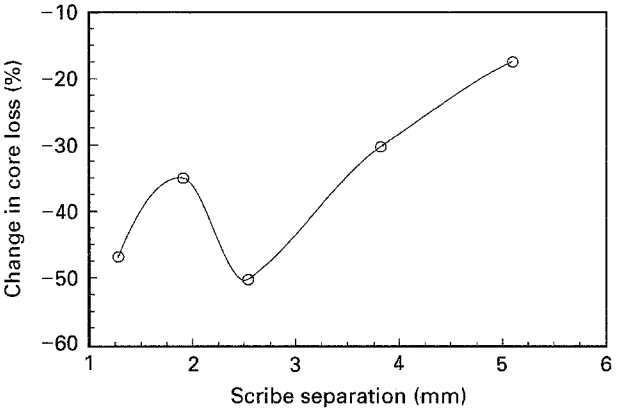

Figure 4 Per cent change in core loss of 3% silicon–steel: longitudinal scribing.

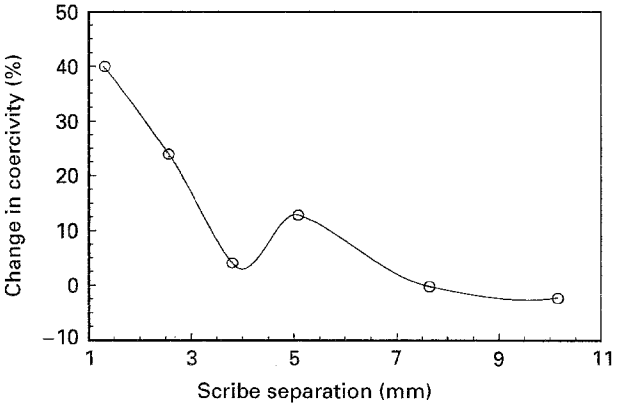

Figure 5 Per cent change in coercivity of 3% silicon–steel: widthwise scribing.

Figs 3–8 show the results obtained in terms of core loss, coercivity and remanence. The per cent change in each property is plotted against the scribe separation distance. The per cent change in the property is calculated by taking the difference in the values before and after laser treatment divided by the original value.

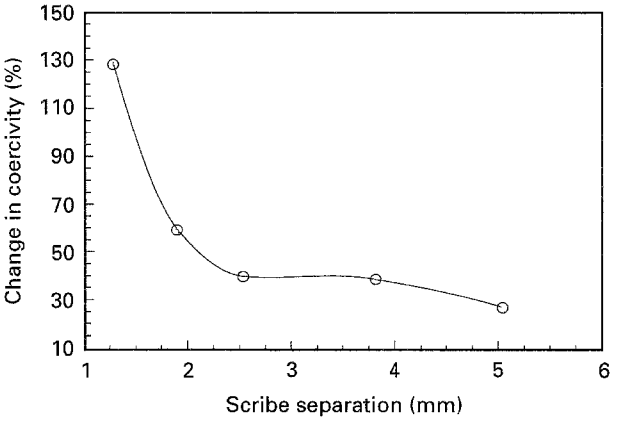

Figure 6 Per cent change in coercivity of 3% silicon–steel: longitudinal scribing.

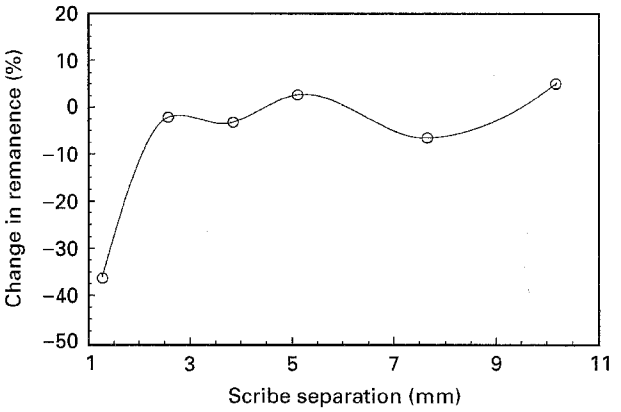

Figure 7 Per cent change in remanence of 3% silicon–steel: widthwise scribing.

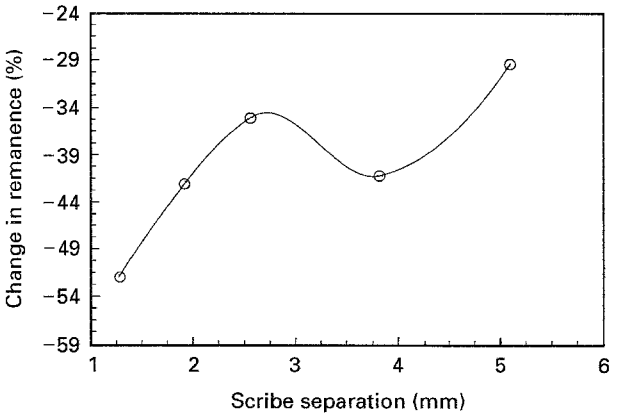

Figure 8 Per cent change in remanence of 3% silicon–steel: longitudinal scribing.

Core loss and remanence decreased overall with a decrease in scribe spacing, while the coercivity increased. The reduction in core loss is primarily due to magnetic domain refinement. The actual physical break-up of the domains dominates any other mechanism, because the excimer laser delivers an almost physical shock rather than a more distributed thermal input like the carbon dioxide or the Nd:YAG laser. The formation of subdomains thus leads to increased magnetic softness. The stresses generated along the

scribe lines also tend to increase the surface resistivity, which results in a reduction in total eddy current loss.

3.2. Nd:YAG laser scribing

Laser scribing of silicon–steel samples was performed with a pulsed Nd:YAG laser. The focal length of the lens was 150 mm, and scribing was carried out under a gentle stream of air from a nozzle. A total of six samples was scribed. Four of these were cut from the rolled sheet along the rolling distance (AS), and the other two were cut perpendicular to the rolling direction (XAS). Pulse repetition frequencies of 5 and 10 Hz were used. The velocity of the X–Y table was either 12.7 or 41.3 mm s^{-1}. These two parameters combined gave a pulse separation distance, Δ, of either 2.54 or 4.1 mm, respectively. The scribe separation distance was kept constant at 1 mm. Table VII shows the data on the laser-processing conditions. Before laser treatment, the samples were characterized in a d.c. field of 14.42 Oe (applied voltage 0.17 A). The hysteresis loss, coercivity, remanence and permeability were measured. Table VII shows the properties of the samples before laser treatment. The effect of laser scribing on the magnetic properties of AS samples is shown in Tables VIII and IX. Table X shows the results of the scribing experiments on the XAS samples. The per cent changes in the magnetic properties after laser treatment are shown. In contrast to the AS samples, XAS samples showed a reduction in the hysteresis loss after laser scribing.

TABLE VII Magnetic properties of silicon steel under d.c. field before laser treatment

Sample	W_c (erg cm^{-3})	H_c(Oe)	B_r(kG)	μ
AS	1931	0.320	7.29	5322.5
XAS	2305	0.465	5.50	2520.0

TABLE VIII Effect (% change) of Nd:YAG laser scribing on AS samples, single-side scribing

Pulse separation (mm)	W_c	H_c	B_r	μ
2.54	+ 8.75%	+ 126.56%	− 59.87%	+ 15.77%
4.10	+ 15.48%	+ 71.87%	− 47.73%	+ 85.53%

TABLE IX Effect (% change) of Nd:YAG laser scribing on AS samples, double-side scribing

Pulse separation (mm)	W_c	H_c	B_r	μ
2.54	+ 6.42%	+ 143.75%	− 63.85%	+ 83.53%
4.10	+ 9.27%	+ 90.62%	− 58.30%	+ 169.64%

The properties of the samples after laser treatment were compared with the average as-received properties. Results indicated that Nd:YAG laser scribing could successfully be applied to 3% silicon–steels. There was no significant difference between the properties of samples scribed on a single side or both sides. On AS samples scribed only on a single side, the hysteresis loss and coercivity were increased to a very large extent. Remanence was decreased and permeability was enhanced. The same effects were observed in samples scribed on both sides, except that the improvement in permeability was more evident in this case. The XAS samples, however, showed a significant reduction in d.c. hysteresis loss. Encouraging results were also obtained with respect to remanence and permeability. The coercivity, however, showed an increase in both the samples. The differences in hysteresis loss between the AS and XAS samples after laser treatment is explained by the 90° difference in orientation of the magnetic domains on the surface of the samples. During laser scribing, the laser beam travels along the length of the sample. Because this direction is perpendicular to the longitudinal axis of the domains in the XAS samples, domain refinement occurs much more easily and to a greater extent than in the AS samples.

In the AS samples, domain refinement does not occur; instead, the laser beam introduces imperfections in the substrate in the form of the boundaries between the laser spots, which are high stress. These regions prevent the reorientation of the domains during magnetization. This is the reason why there was an increase of hysteresis loss and coercivity. However, the stresses introduced may also result in the breakage of bonds in the lattice structure of the substrate, leading to relaxation of internal strains. This is believed to be the reason for the increase in permeability.

In the case of the XAS samples, the reduction in hysteresis loss is accompanied by an increase in coercivity. Although the refinement of domains occurs, stresses are introduced at the same time on the surface of the samples just as in the AS samples. Because these stresses tend to keep the domains in a state of high compression, the magnetic field needed to reduce the magnetization to zero is considerably more than that in the absence of stress. The tensile stresses generated as more laser scribe lines are introduced, are probably insufficient to eliminate completely these compressive stresses, because they are localized in a very small region around the laser spot. The increase in permeability is a result of the domain refinement. Smaller domains tend to get magnetized and demagnetized much more easily. Thus, remanence and permeability are decreased and increased, respectively, as a result of laser scribing.

TABLE X Results (% change) of Nd:YAG laser scribing of XAS samples

Samples	Sides scribed	W_c	H_c	B_r	μ
XAS4	One	− 11.5%	+ 64.50%	− 49.2%	+ 92.85%
XAS5	Both	− 12.6%	+ 80.64%	− 54.1%	+ 60.51%

3.3. Carbon dioxide laser scribing

The experimental parameters were listed in Table XI. Laser power and the scribe separation were varied and all other parameters were kept constant. The focal length of the lens was 0.127 m. Argon was used as the assist gas. Laser power levels of 50 and 200 W were used. However, the results showed that 200 W laser power degraded the material properties. Hence, this power level was not used in subsequent experiments.

Table XII shows the results of the laser scribing experiments, performed on four samples, XAS 27–30. The variation of core loss of the silicon steel samples after scribing with the CO_2 laser is shown in Figs 9–11. The plots show core loss as a function of the induction level and scribe separation distance.

Results indicated that CO_2 laser scribing of 3% silicon–steel was effective in improving the magnetic properties of samples tested. It can be seen from Fig. 9 that there has been a substantial decrease in core loss at all the induction levels investigated, namely from 0.8 T to 1.1 T. This decrease in core loss ranged from 36% for XAS 27 at 0.9 T to as much as 64% for XAS 28 at 0.9 T. In both cases, the per cent reduction in the hysteresis loop area shows a decreasing trend with increasing induction level, with XAS 28 showing a steeper fall. This suggests that the mechanism of core-loss reduction is related to the magnetic induction induced in the sample. On the other hand, Fig. 10 shows an initial increase in core loss with magnetic induction for samples XAS 29 and XAS 30. But it can clearly be seen that for samples XAS 29 and 30, there is a consistent downward trend in the core loss with increasing magnetic induction. Sample XAS 30 showed the maximum increase of 41%. Although a quantitative explanation of the complex behaviour of silicon–steels towards laser scribing is not available at present, an attempt is made here to obtain a qualitative understanding of the laser scribing process and its effect on the magnetic properties of silicon–steels.

Because laser scribing induces magnetic domain refinement, the subdomains so formed are much more easily magnetized than the larger main domains. Also, because all the samples are of the XAS type, the main domains as well as the subdomains are oriented perpendicular to the longitudinal axis of the samples. When the samples are magnetized in the solenoid, the

TABLE XI CO_2 laser scribing of 3% silicon–steel

Laser	Continuous wave CO_2 (10 600 nm)
Power (W)	50, 200
Speed of X–Y table (mm s^{-1})	170
Scribe direction	Longitudinal (L)
Scribe separation distance, Δs (mm)	1.27, 2.54, 5.08
Sample dimensions (mm)	304.8 × 30 × 0.23
Domain orientation	XAS

TABLE XII CO_2 laser scribing of silicon steel

Sample	Induction (T)	*B–H* loop area		Change
		Before (cm^2)	After (cm^2)	
XAS 27	0.9	5.9045	3.7832	− 36%
XAS 27	1.0	7.5122	4.4122	− 41%
XAS 27	1.1	9.9722	4.7728	− 52%
XAS 28	0.8	6.7464	3.6958	− 45%
XAS 28	0.9	12.0503	4.2645	− 64%
XAS 29	0.9	3.3032	4.1877	+ 27%
XAS 29	1.1	4.4503	5.4130	+ 22%
XAS 29	1.4	6.4300	5.6967	− 11%
XAS 30	0.9	3.2038	4.5325	+ 41%
XAS 30	1.1	4.3742	5.9483	+ 36%
XAS 30	1.4	6.7793	7.5671	+ 12%

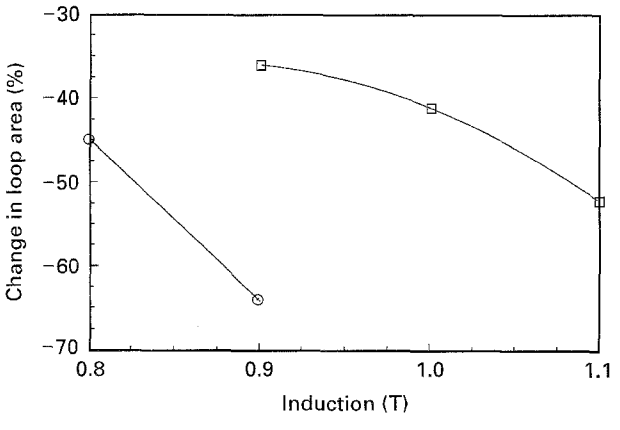

Figure 9 Variation of core loss of 3% silicon–steel: (□) XAS 27, (○) XAS 28.

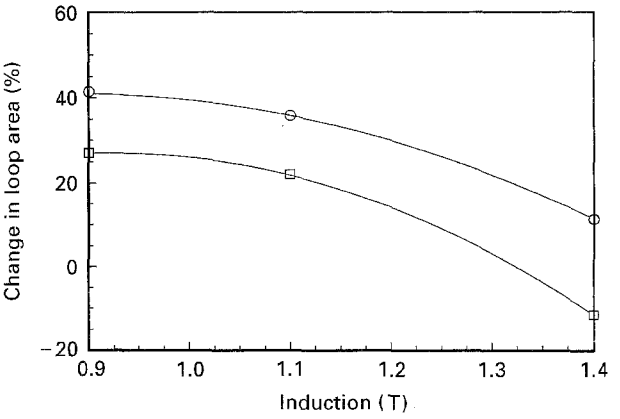

Figure 10 Variation of core loss of 3% silicon–steel: (□) XAS 29, (○) XAS 30.

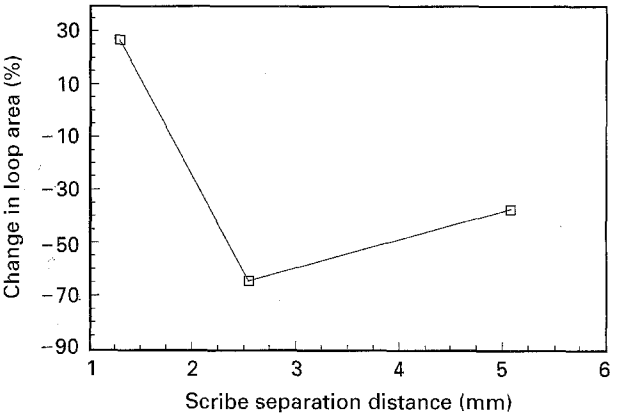

Figure 11 Effect of scribe separation distance on core loss for 0.9 T.

magnetic field induced is also oriented along this direction. Hence, it becomes progressively easier to magnetize the samples with increasing induction levels. As the magnetic induction is increased, the number of subdomains oriented parallel to the magnetic field increases, and saturation is attained at lower fields. With growing ease of magnetization, the core loss also decreases. The initial positive change in the loop area for samples XAS 29 and 30 maybe due to minor variations in the properties of the rolled steel inherent in the manufacturing process.

Fig. 11 shows the variation of core loss as a per cent change with scribe separation distance. It can be seen that the maximum reduction in the loop area occurs for a scribe separation distance of between 2 and 3 mm for an induction of 0.9 T. On either side of this range, the core loss rapidly rises. This means that the optimum scribe separation distance lies in the range specified above.

At a scribe separation distance of between 2 and 3 mm, the size of subdomains formed is at a minimum. The stress relaxation is maximum. Tensile stresses created between the laser scribe lines not only overcome the compressive stresses induced in the plastically deformed zone, but refine the main domain-wall spacing. Because the domains are oriented perpendicular to the length of the samples, the tensile stresses elongate the main domains, thus decreasing the space between the domain walls. This elongation also removes supplementary domain structures, making for a more uniform and homogeneous subdomain structure after laser scribing. The increase in core loss at other scribe spacings seems to be due to inhomogeneities introduced in the domain structure of the samples by the thermal input of the laser beam. The inhomogeneities may be in the form of distortions in the domain structure, pinning sites formed by resolidified melt pools, or insufficient domain refinement due to large scribe spacing.

3.4. Summary

The effect of each laser on the magnetic properties of 3% silicon steel is rated on a scale of A to C, A denoting the most favourable effect and C indicating the least favourable. The ratings are shown in Table XIII.

Neiheisel and Schoen [9, 10] demonstrated that Nd:YAG laser shock-hardening treatment of transformer core, grain-oriented silicon–iron alloys having an insulative coating reduced the core losses without damaging the coating. This was also followed-up by Nakamura *et al.* in Japan [11], who studied the effect of laser irradiation on the domain structure and magnitude of the plastic deformation induced on the surface of grain-oriented silicon–steel samples. A Q-switched Nd:YAG laser with a focused spot size of 0.12 mm and an energy per pulse of 3.75 mJ was used. It was found that the domain structure was refined along the lines irradiated by the laser. These new subdomains were oriented differently from the 180° magnetization direction of the main domains. The 180° domain-wall spacing was not affected by a single laser spot line. However, it was refined when more laser spot lines were added beside the first irradiated line. These changes in the domain structure were attributed to the tensile stresses induced by the laser pulses in the substrate. The amount of plastic deformation in the irradiated sample was found to be at least equal to 10% strain during tensile deformation.

TABLE XIII Laser scribing of 3% silicon steel: summary of results

Property	Excimer	Nd:YAG	CO_2
W_c	A	B	A
μ	C	A	–
H_c	B	C	–
B_r	B	A	–

The modification of local magnetic properties on steel surfaces due to laser irradiation was investigated by Fuh [12]. The objective was to induce "ripple patterns" on the steel surface and study the changes in the magnetic properties due to these patterns. Two samples of 304 stainless steel and one sample of chromium-coated cold-rolled steel were used in this study. A Q-switched Nd:YAG laser with an average pulse width of 100 ns focused by a Glan-Taylor prism to obtain linearly polarized light, was used to irradiate the samples. The focused spot size on the sample surface was about 0.2 mm diameter. The repetition rate of the laser was less than 1 Hz. It was found that the induced ripple structure was dependent only on the number of laser pulses incident on the surface. Pronounced ripple patterns were obtained with about 10 pulses, each having an energy of 0.35 J cm^{-2}. The results demonstrated that although ripple patterns were produced on all the samples, the changes in the local magnetic properties were significant only in the chromium-coated sample. This was believed to be due to the diffusion of chromium atoms into the substrate material, thus transforming it locally into a non-magnetic stainless steel.

A similar study was also performed by Iuchi *et al.* [13]. Again, a Q-switched Nd:YAG laser was used to irradiate samples of grain-oriented silicon steel. The energy per pulse was 3.75 mJ, and the focused spot size was 0.15 mm. The spots on the surface of the samples hit by the laser beam were found to refine the 180° domain-wall spacing and reduce the core loss by as much as 10% under optimum conditions of laser processing.

In the present study, three mechanisms are postulated in order to explain the increase in magnetic softness of magnetic materials after laser treatment. These are: (1) magnetic domain refinement, (2) relaxation of internal stress, (3) inhibition of domain wall movement.

3.4.1. Magnetic domain refinement

Subdomains are formed when the energy input from the laser beam breaks bonds on the substrate and sets domains free. The extremely high concentrtion of laser energy also plastically deforms the substrate, forming a localized zone of compressive stress. Both

the free poles and the plastic zone tend to increase the magnetoelastic energy, leading to increased anisotropy. To offset this increase, subdomains are formed which orient themselves with a positive and negative pole at either end, so as to combine the free poles into a single domain [11]. Magnetoelastic energy is also decreased by the formation of subdomains in the plastically deformed zone. As the number of laser scribe lines increases, tensile stresses are created between the lines, reducing the magnetoelastic energy. As a result, the size and number of subdomains decrease, resulting in a refinement of the 180° main domain-wall spacing.

3.4.2. Relaxation of internal stress

Internal stress relaxation is an effect of the domain-refinement mechanism. The concentrated heat input from the laser beam leads to breakage of bonds as the domains are refined. The breakage of bonds releases the internal strains frozen-in during manufacture of the material, producing stress relaxation. The compressive stresses induced in the plastically deformed zone are overcome by the tensile stresses between the laser scribe lines. This may also produce relaxation of the compressive stresses induced during rolling of the material. As the stress decreases, the magnetoelastic energy also decreases, and the magnetic softness increases.

3.4.3. Inhibition of domain-wall movement

The absorbed energy vaporizes the silicate and phosphate coating on the sample together with a thin layer of the substrate material, forming a groove on its surface. Material from the sides of this groove forms melt pools which later resolidify. These resolidified melt pools form pinning sites between the magnetic domains. This inhibits domain-wall movement during the magnetizing and demagnetizing cycles. They also physically break up the domains. The resultant stress fields on the surface also inhibit the movement of the domain walls, leading to increased surface resistivity. Now the total eddy current loss, equal to the sum of the classical eddy current loss and the anomalous eddy current loss, is related to the resistivity by

$$P_e = \mu f/R \qquad (1)$$

where P_e is the total eddy current loss, μ the permeability, f the frequency, and R the resistivity. The increased surface resistivity decreases the total eddy current loss, thus decreasing the total core loss.

4. Conclusion

Laser scribing of 3% silicon–steel was carried out with the objective of enhancing the magnetic properties. Three types of lasers were used in the experimental work, a 248 nm, pulsed KrF excimer laser, a 10 600 nm continuous wave carbon dioxide laser, and a 1064 nm pulsed Nd:YAG laser. The laser-processing parameters included the energy density at the surface of the workpiece, pulse repetition rate (if a pulsed laser), pulse separation distance (for a pulsed laser) and scan separation distance. The magentic properties tested included hysteresis loss, total core loss, coercivity, remanence, permeability and saturation induction. The samples were characterized before and after laser treatment in both a.c. and d.c. fields to evaluate the effect of laser annealing and scribing on the magnetic properties. The principal results and conclusions are as follows.

In excimer laser scribing of silicon–steel, results showed an overall decrease of hysteresis loss with decreasing scribe spacing. There was no apparent difference whether the scribing direction was widthwise or longitudinal. However, the coercivity increased with decreasing scribe spacing. Remanence also followed the same trend as core loss. Permeability increased with pulse energy up to a threshold value, after which it decreased. Even though the decrease in core loss, and, in some cases, the decrease in remanence is a positive result, the corresponding increase in coercivity offsets it. The reduction in core loss and remanence is due to the magnetic domain refinement that occurs. The size of the domains is physically reduced by the shock action of the excimer laser. The smaller domains are better able to orient themselves along an applied magnetic field, and thus respond more efficiently to changing fields. Moreover, the groove scribed on the sample surface increases the surface resistivity, and because this is inversely related to the eddy current loss, core loss is reduced. Improvement of overall efficiency is thus obtained.

Nd:YAG laser scribing of 3% silicon–steel improved d.c. hysteresis loss and permeability. This is accompanied by a decrease in remanence and an increase in coercivity. Reduction in hysteresis loss was only observed in XAS samples. Coercivity increased in both AS and XAS samples, as did permeability. Remanence decreased in both types of sample. The maximum reduction in hysteresis loss was about 12%. Although these are encouraging results, the experiments need to be repeated in order to confirm the results, because the variation in the as-received properties of the samples was much too large. This laser can thus be used only in cases where the increase in coercivity and decrease in remanence are not critical to the performance of the material.

The final part of this study focused on the carbon dioxide laser scribing of silicon–steels and its effect on the total core loss. Scribing direction was always perpendicular to the rolling direction. The samples showed a consistent decrease in core loss with increasing induction level and decreasing scribe separation. Magnetic domain refinement results in the formation of subdomains that are magnetized much more easily than the larger main domains. Laser scribing also causes refinement of the 180° main domain-wall spacing. As a result, the domain structure as a whole becomes more homogeneous, suppressing such effects as domain-wall bowing and distortion during magnetization. The optimum scribe separation distance was in the range of 2–3 mm, approximately. On either side of this range, the core loss increased. Maximum domain refinement and stress relaxation is believed to

occur in this range. The tensile stresses formed between the scribe lines elongate the domains and refine the wall spacing. At closer scribe spacing, the compressive stresses generated in the plastically deformed zone are probably too high to be overcome by the tensile stresses. At wider scribe spacing, sufficient domain refinement probably does not occur.

Acknowledgements

The authors acknowledge the financial support provided by the Electric Power Research Center of Iowa State University. The authors thank the Magnetics Group of Ames Laboratory, US Department of Energy, Ames, Ia, for the use of the magnescope and other measuring equipment, and for assistance in characterization of the samples. The authors also acknowledge the materials support provided by Asea Brown Boveri Technology Corp., Raleigh, NC.

References

1. R. M. WHITE, *Science* **229** (4708) (1985) 11.
2. H. WARLIMONT, *IEEE Trans. Mag.* **26** (1990) 1313.
3. G. BERTOTTI and M. PASQUALE, *ibid.* **28** (1992) 2787.
4. F. FIORILLO and A. NOVIKOV, *ibid.* **26** (1990) 2559.
5. K. C. LIN and E. E. ZOOK, *J. Mater. Eng.* **11** (1989) 117.
6. D. C. JILES, "Introduction to Magnetism and Magnetic Materials" (Chapman and Hall, New York, NY, 1991).
7. A. J. MOSES, *IEEE Proc.* **137** (1990) 233.
8. DOUGLAS W. DIETRICH, "Metals Handbook", Vol. 2, 10th Edn (The American Society for Metals,Cleveland, OH, 1990) p. 761.
9. G. L. NEIHEISEL, *SPIE* **668** (1986) 116.
10. G. L. NEIHEISEL and J. W. SCHOEN, Unpublished paper presented at the Conference on Lasers and Electro-Optics (CLEO '84) Anaheim, CA, 19–22 June (1984).
11. M. NAKAMURA, *et al.*, *IEEE Trans. Mag.* **23** (1987) 3074.
12. ANDY Y. G. FUH, *Appl. Phys.* **A 54** (1992) 176.
13. T. IUCHI, S. YAMAGUCHI, T. ICHIYAMA, M. NAKAMURA, T. ISHIMOTO and K. KUROKI , *J. Appl. Phys.* **53** (1982) 2410.

Received 2 February
and accepted 4 October 1995